

$$P(\theta) = \frac{2}{X} \left[e^{-ZX}(1-Z) - \frac{1}{X}(e^{-ZX} - e^{-X}) \right] + \frac{Z}{\nu Y^{1/2\nu}} \left[\gamma\left(\frac{1}{2\nu}, Y\right) - \frac{Z}{Y^{1/2\nu}} \gamma\left(\frac{1}{\nu}, Y\right) \right] \quad (12)$$

where X and γ have the same definitions as in eq 5 but Z is an adjustable parameter between 1 and 0 and $Y = ZX$. This equation agrees with eq 1 if $Z = 0$ and with eq 3 if $Z = 1$. At an intermediate value of Z , eq 12 describes the Debye function form (eq 1) in the low q range and the Peterlin function form (eq 3) in the high q range. Equation 12 happens to be the same as eq 3.8 of ref 9 in the blob theory for a polymer chain in semidilute solutions. However, their physical meanings are different; $\langle s^2 \rangle$ is expected to increase in proportion to N in semidilute solutions, whereas the experimental values, which are proportional to $N^{1+\epsilon}$, are inserted into $\langle s^2 \rangle$ for an isolated polymer in good solvents.

Assuming that Z is an adjustable parameter and $\nu = 0.6$, we evaluated $P(\theta)$ from eq 12 and compared them with experimental data. As shown in Figure 5, satisfactory agreement between the calculated and experimental values is obtained if we assume $Z = 0.05$.

As explained in the Introduction, $P(\theta)$ of poly(sodium acrylate), on the other hand, in the presence of an added salt agrees with eq 3 over the entire range of q . This means that $Z = 1$ in eq 12 for polyelectrolytes. Although the interaction between nonionic segments and the electrostatic interaction between charged groups are both considered to be excluded volume effects, the former may drop much more rapidly than the latter. Moreover, the same data are replotted in the form of eq 7 in Figure 4B. The slopes at high q can give values higher than 0.6 for ν , i.e., higher than 0.2 for ϵ , at low ionic strengths.

Finally, it is to be noted that the interpenetration function $\Psi(\bar{z}) (= A_2 M^2 / 4\pi^{3/2} N_A \langle s^2 \rangle^{3/2})$ calculated from the

data in Table I is found to be 0.24, 0.21, and 0.23 for $M = 0.84 \times 10^7$, 1.1×10^7 and 2.1×10^7 , respectively. This result agrees with our previous conclusion that $\Psi(\bar{z})$ converges to 0.2₁ as the molecular weight increases^{3,17} and also with the data reported later.^{16,18}

Acknowledgment. We thank the Ministry of Education, Science and Culture, Japan, for financial support through a Grant-in-Aid for Scientific Research (Grant 347079).

Registry No. Polystyrene, 9003-53-6.

References and Notes

- (1) School of Material Science, Toyohashi University of Technology, Tempaku-cho, Toyohashi, Japan 440.
- (2) Debye, P. *J. Phys. Colloid Chem.* **1947**, *51*, 18.
- (3) Kato, T.; Miyaso, K.; Noda, I.; Fujimoto, T.; Nagasawa, M. *Macromolecules* **1970**, *3*, 777.
- (4) Kitano, T.; Taguchi, A.; Noda, I.; Nagasawa, M. *Macromolecules* **1980**, *13*, 57.
- (5) Nagasawa, M.; Noda, I.; Kitano, T. *Biophys. Chem.* **1980**, *11*, 435.
- (6) Peterlin, A. *J. Chem. Phys.* **1955**, *23*, 2464.
- (7) Ptitsyn, O. B. *Zh. Fiz. Khim.* **1957**, *31*, 1091.
- (8) Benoit, H.; C. R. *Hebd. Seances Acad. Sci.* **1957**, *245*, 2244.
- (9) Farnoux, B.; Boue, F.; Cotton, J. P.; Daoud, M.; Jannink, G.; Nierlich, M.; de Gennes, P.-G. *J. Phys. (Paris)* **1978**, *39*, 77.
- (10) Francois, J.; Schwartz, T.; Weill, G. *Macromolecules* **1980**, *13*, 564.
- (11) Mazur, J.; McIntyre, D. *Macromolecules* **1975**, *8*, 464.
- (12) Smith, T. E.; Carpenter, D. K. *Macromolecules* **1968**, *1*, 204.
- (13) Fujita, H. *Polym. J.* **1970**, *1*, 537.
- (14) Fujimoto, T.; Nagasawa, M. *Polym. J.* **1975**, *7*, 397.
- (15) Norberg, P. N.; Sundelöf, L. O. *Makromol. Chem.* **1964**, *77*, 77.
- (16) Miyaki, Y.; Einaga, Y.; Fujita, H. *Macromolecules* **1980**, *11*, 1180.
- (17) Noda, I.; Kitano, T.; Nagasawa, M. *J. Polym. Sci., Polym. Phys. Ed.* **1977**, *15*, 1129.
- (18) Fukuda, M.; Fukutomi, M.; Kato, Y.; Hashimoto, T. *J. Polym. Sci., Polym. Phys. Ed.* **1974**, *12*, 871.

Small-Angle X-ray Scattering Study of Density Fluctuation in Polystyrene Annealed below the Glass Transition Temperature

Ryong-Joon Roe* and J. J. Curro

Department of Materials Science and Metallurgical Engineering,
University of Cincinnati, Cincinnati, Ohio 45221. Received July 12, 1982

ABSTRACT: The intensity of X-rays scattered at small angles provides a measure of the density fluctuation in amorphous solids. Above T_g the density fluctuation is thermally induced and proportional to compressibility, while below T_g it has in addition a contribution from frozen-in inhomogeneities. When polystyrene was annealed below T_g , the observed behavior depended on the annealing temperature. Between 80 and 100 °C the density fluctuation decreased approximately linearly with the logarithm of time, while below 80 °C it remained constant in the 24-h observation period. On constant-rate cooling, the observed density fluctuation against temperature could be represented by three linear sections, the liquid line above T_g , the glass line below about 80 °C, and a transition line between about 80 and 100 °C. Three narrow fractions of 17500, 220000, and 1800000 molecular weight and a commercial sample were studied and were observed to give a density fluctuation in glass that depended sensitively on molecular weight. The behavior of the density fluctuation on isothermal annealing, on constant-rate cooling, and on changing molecular weight is very different from the behavior of specific volume under similar conditions. Whereas the specific volume might provide a measure of the average free volume content, the density fluctuation can be interpreted to reveal the distribution of free volume. The small-angle X-ray scattering measurement thus offers a glimpse into the structure of glass from a very different angle of view and would prove a valuable tool in our efforts to understand the nature of glass.

I. Introduction

When a glassy material is annealed at temperatures moderately below its glass transition temperature, its internal structure undergoes a slow relaxation toward

equilibrium. This structural relaxation can be demonstrated through measurements of various properties, for example, specific volume,¹ heat content,² and creep properties.³ Each of these properties provides a "window"

through which a particular glimpse of the underlying molecular processes is obtained. A more complete understanding of these molecular processes is likely through simultaneous measurements of different properties. In this work, we study relaxation of the density fluctuation by means of the small-angle X-ray scattering technique and compare the results with those obtained from volume relaxation measurements.

Scattering of X-rays at small angles from an amorphous, single-phase, single-component material arises from the presence of electron density fluctuation caused by the irregular, liquid-like placement of atoms. In the case of an equilibrium liquid, the extent of this density fluctuation is related to the isothermal compressibility β_T , and the intensity $I(s)$ extrapolated to $s = 0$ ($s = (2 \sin \theta)/\lambda$) is given⁴ by

$$I(0) = kT\rho^2\beta_T \quad (1)$$

where ρ is the average electron density and $I(0)$ is expressed in electron units per unit volume. A number of workers⁵⁻¹² have shown that eq 1 is obeyed well by polymer liquids above their glass transition temperatures.

Below T_g eq 1 is no longer expected to hold since a glass is in a nonequilibrium state. In fact, when the observed compressibility β_T^g of the glass is substituted for β_T in eq 1, the predicted $I(0)$ is much lower than the observed value.^{5,10-12} Equation 1 denotes the magnitude of dynamic density fluctuation induced by thermal energy kT working against bulk compliance β_T . The observed $I(0)$ for glasses, much larger than predicted by eq 1, suggests that the density fluctuation in glasses includes a contribution from static fluctuation¹⁰ that was frozen in during, and possibly subsequent to, the glass formation. Thus, the density fluctuation of glassy polymers may depend upon the history of formation of the glass and also may change with time when annealed below T_g . To address these questions, in this work we study four polystyrene samples by measuring the change in the density fluctuation on constant-rate heating and cooling and on isothermal annealing at temperatures moderately below T_g .

II. Density Fluctuation

Consider a reference volume v of arbitrary shape and size. As we move this reference volume around in the sample, the number N of electrons falling within the volume will fluctuate about the mean $\langle N \rangle$. The density fluctuation $\psi(v)$ is defined by

$$\psi(v) = \langle (N - \langle N \rangle)^2 \rangle / \langle N \rangle \quad (2)$$

where the angular brackets denote a spatial average over the sample (or the scattering volume).

In general $\psi(v)$ depends only weakly on v . In the case of a random assemblage of points in space, the probability $P(N)$ of finding N points in v is given by a Poisson distribution:

$$P(N) = (\rho v)^N \exp(-\rho v) / N! \quad (3)$$

where ρ is the average density. In this case $\psi(v)$ is equal to unity for all v . To gain a feel for the meaning of the dependence of $\psi(v)$ on v , we consider the following examples. Suppose that the probability of finding N electrons in a reference volume v of a certain size, say v_1 , is given by a distribution function $P_1(N)$ of mean ρv_1 and variance σ^2 . The density fluctuation $\psi(v_1)$ is equal to $\sigma^2/\rho v_1$. Next consider a reference volume $v_2 = 2v_1$ which can be formed by joining two neighboring volumes of v_1 each. The probability $P_2(N)$ of finding N electrons in volume v_2 can be given by a convolution product of two $P_1(N)$'s, provided

that the probability distributions of electrons in the neighboring volumes are mutually independent. If this is the case, then the mean and the variance of $P_2(N)$ are equal to ρv_2 and $2\sigma^2$, and $\psi(v_2)$ is given by $\sigma^2/\rho v_1 = \psi(v_1)$. By repeating the same argument, we conclude that $\psi(v)$ is invariant for all v greater than v_1 . Next consider a reference volume v half the size of v_1 . If, on dividing v_1 into two halves, the probability of finding N electrons in the second half is not influenced by the knowledge of the number of electrons in the first half, then the density fluctuation $\psi(v_1/2)$ should be equal to $\psi(v_1)$. As the reference v is further reduced, a point is eventually reached at which the electron density between neighboring volumes is no longer independent, and $\psi(v)$ ceases to be independent of v . The above geometric interpretation shows that $\psi(v)$ will in general be independent of v as long as the linear scale of v exceeds the distance of atomic correlation due to intermolecular forces.

The intensity of scattered X-rays is determined by the spatial distribution of electrons in the sample. Cu K α radiation of $\lambda = 1.54 \text{ \AA}$ takes $5 \times 10^{-19} \text{ s}$ for one wave period, which is several orders of magnitude shorter than the time period of atomic motions. The scattering of X-rays is therefore unaffected by atomic motions, and the scattered intensity arising from density fluctuation remains the same irrespective of whether the fluctuation is dynamic or static.

The intensity $I(s)$ of X-rays scattered by a unit volume in the direction s is related to the density fluctuation $\psi(v)$, according to Ruland,¹⁰ by

$$\psi(v) = \int \frac{1}{\rho} I(s) \frac{1}{v} [\Phi(s)]^2 ds \quad (4)$$

where $\Phi(s)$ is the Fourier transform of the form factor of the reference volume v . As shown later, the observed intensity scattered from polystyrene (both above and below T_g) can be approximated well by

$$I(s) = I(0) \exp(bs^2) \quad (5)$$

where b is an empirical constant. Equation 5 was shown to be obeyed also by some other polymers and liquids.¹¹ Substitution of (5) into (4) gives (see Appendix)

$$\psi(v) = \psi(\infty) / (1 - b/\pi v^{2/3})^{3/2} \quad (6)$$

with

$$\psi(\infty) = \lim_{s \rightarrow 0} (1/\rho) I(s) \quad (7)$$

Thus, $\psi(v)$ is practically independent of v when v is large in comparison to $b^{3/2}$ and increases only moderately when v is decreased to a fairly small size. With b equal to 1.3 nm^2 , appropriate to our polystyrene data, $\psi(v)$ for $v = 8 \text{ nm}^3$ is about 18% larger than $\psi(\infty)$.

For liquids in thermal equilibrium, the theory of statistical thermodynamics shows that

$$\psi(\infty) = \rho k T \beta_T \quad (8)$$

With glassy materials the observed density fluctuation consists of a dynamic and a quasi-static component:

$$\psi_{\text{obsd}}(v) = \psi_{\text{dyn}}(v) + \psi_{\text{qst}}(v) \quad (9)$$

Here, $\psi_{\text{qst}}(v)$ represents the density fluctuation that is frozen in, while the dynamic component $\psi_{\text{dyn}}(v)$ is related to the compressibility of the glass, β_T^g , by

$$\psi_{\text{dyn}}(\infty) = \rho k T \beta_T^g \quad (10)$$

in analogy to eq 8. Even in glasses, there are many degrees of freedom with relaxation times much shorter than the experimental time scale, and these fast modes can attain

thermal equilibrium within the constraints imposed by the frozen structure. Equation 10, which describes the component of the density fluctuation due to such fast modes, should be valid as long as the time scales of measurement of compressibility and of density fluctuation are comparable.

A more detailed justification of eq 9 and 10 can be given from a statistical mechanical consideration of an "ideal" glass. The notion of a "perfect glass" or a "theorist's ideal glass" was suggested by Edwards.¹³ In any ideal glass, quenched from a temperature $T_0 > T_g$ to $T_1 < T_g$, atomic and molecular motions are assumed to belong distinctly to either fast or slow modes. Those motions belonging to slow modes are virtually frozen, while the fast modes readily attain thermal equilibrium. The grand canonical ensemble representing such an "ideal" glass then subdivides itself into a set of subensembles, each representing a particular frozen-in configuration of the glass. Within each subensemble a thermal equilibrium is maintained and the equilibrium statistical mechanics is applicable. As described elsewhere,¹⁴ a detailed consideration of density fluctuation in such an "ideal" glass leads to a more rigorous justification of eq 9 and 10, as well as to a clarification of the meaning of the terms dynamic and quasi-static fluctuations.

III. Experimental Section

Four polystyrene samples were studied. The anionically polymerized samples, obtained from Pressure Chemical Co., are of molecular weight 17 500, 233 000, and 1 800 000; the first two are claimed to have M_w/M_n ratios less than 1.06 and the third an $M_w/M_n < 1.10$. A commercial polystyrene, specially prepared to contain no additives, was obtained from Monsanto Co., and its viscosity-average molecular weight, determined in cyclohexane solution at 35 °C, is 215 000.

Small-angle X-ray scattering measurements were performed with a Kratky camera with Ni-filtered Cu radiation from a Philips XRG3100 generator operating at 45 kV and 40 mA. The Kratky camera was modified¹⁵ for use with a one-dimensional position-sensitive detector. Since the scattered intensity varied very slowly with scattering angle, thus making a good angular resolution unimportant, a wide entrance slit of 300- μ m width was used in order to enhance the intensity of the scattered beam. The stability of the incident X-ray beam power was monitored by means of a separate scintillation counter mounted to receive some stray scattering from the collimating system. The intensity data obtained from the samples were scaled to absolute units by comparison with scattering from a calibrated Lupolen sample¹⁵ kindly supplied by Professor O. Kratky.

The polystyrene sample was compression molded into a cavity in an aluminum sample holder, which was heated by means of cartridge heaters. Two thermocouples were placed close to the sample; one of them was used as a sensor for the temperature controller, and the output from the other was continually recorded on a chart recorder. The temperature regulation was achieved to within ± 0.1 °C, and the temperature jump from 120 to, for example, 80 °C was essentially completed within about 3 min. All the thermal treatment, such as constant-rate cooling and heating and isothermal annealing, was performed while the sample was kept in the camera under vacuum.

Figure 1 shows two examples of the observed intensity data, after correction¹⁵ for the nonuniformity of the detector efficiency along its length. The logarithm of the slit-smear intensity $\tilde{I}(s)$ plotted against s^2 shows a good linear relation. The intensity $\tilde{I}(s)$, corrected for the slit-length smearing effect, is related to $I(s)$ by

$$\tilde{I}(s) = \int_{-\infty}^{\infty} W(t) I(s^2 + t^2)^{1/2} dt \quad (11)$$

where $W(t)$ is the slit-length weighting function. When $\tilde{I}(s)$ can be approximated by $\tilde{I}(0) \exp(bs^2)$, $I(s)$ is also given by $I(0) \exp(bs^2)$, and $\tilde{I}(0)$ and $I(0)$ are related by

$$\tilde{I}(0) = I(0) \int_{-\infty}^{\infty} W(t) \exp(bt^2) dt \quad (12)$$

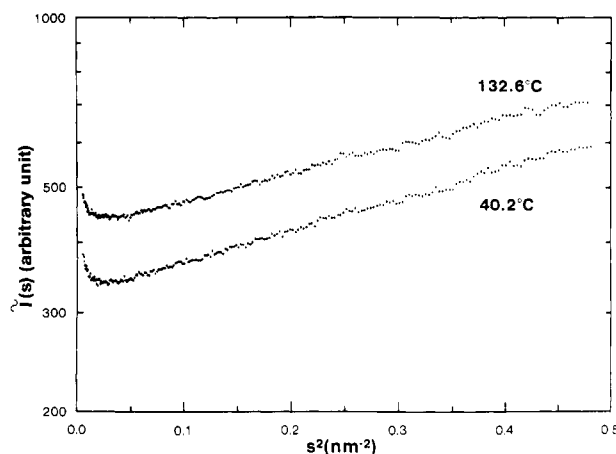


Figure 1. Slit-smear intensity $\tilde{I}(s)$, obtained with the 233 000 molecular weight fraction at 132.6 and 40.2 °C, is plotted to show that $\ln \tilde{I}(s)$ is approximately linear with s^2 for most of the angular range.

Once properly calibrated, the value of $I(0)$ can be obtained from the measurement of $\tilde{I}(s)$ at any arbitrary angle. This is especially true since the shape of the scattering curve does not change measurably with either temperature or time. An empirical relationship correlating $I(0)$ to the observed intensity $\tilde{I}(s)$ integrated from $s = 0.2$ to 0.7 nm^{-1} was first established by calibrating it at several temperatures above and below T_g . Determination of $I(0)$ could then be accomplished by measuring the scattered intensity curve for only 200 or 300 s and then summing the numbers of counts on the multichannel analyzer over the channels corresponding to the required angular range. Because of the large number of counts included in the integrated intensity, the error due to statistical fluctuation was minimized, and the precision of $I(0)$ values attained was much higher than would have been obtained if $I(0)$ were instead evaluated each time by extrapolation of the scattered intensity. In a separate study it was also established that during isothermal annealing the shape of the scattered intensity curve remained the same even while the overall intensity decreased measurably, so that the calibrated relationship could still be used.

IV. Results and Discussion

Figure 2 shows the changes in $I(0)$ observed when the sample was at first cooled from above T_g to room temperature at a rate of 0.3 °C/min and subsequently reheated at 0.5 °C/min. (During the 300-s period while the X-ray intensity was collected, the temperature changed by 1.5 and 2.5 °C, and the points in Figure 2 are plotted on the midpoint of the temperature range.) Figure 2a was obtained with the 233 000 molecular weight fraction and Figure 2b with the commercial polystyrene. A hysteresis loop around T_g is seen clearly in both cases. Shown in Figure 3, for comparison, is the specific volume of the 233 000 molecular weight fraction determined dilatometrically at the same 0.3 °C/min cooling rate. Although the overall features are similar, there are many differences in detail. Linear extrapolations of the specific volume above and below T_g intersect at 97 °C, and the observed specific volume around T_g deviates from these extrapolated straight lines over only a fairly narrow temperature range 91 – 103 °C. For $I(0)$ observed on cooling the 233 000 molecular weight fraction, extrapolations of liquid and glass lines intersect at ca. 92 °C, and the transition region around T_g , in which the observed values deviate from the extrapolated lines, now extends over a 30 °C range. The $I(0)$ values in the transition region in fact follow a straight line of their own, and at its low-temperature end the temperature coefficient changes over fairly abruptly to that of the glassy state. When the straight lines in the glassy, transition, and liquid regions in Figure 2a are extrapolated

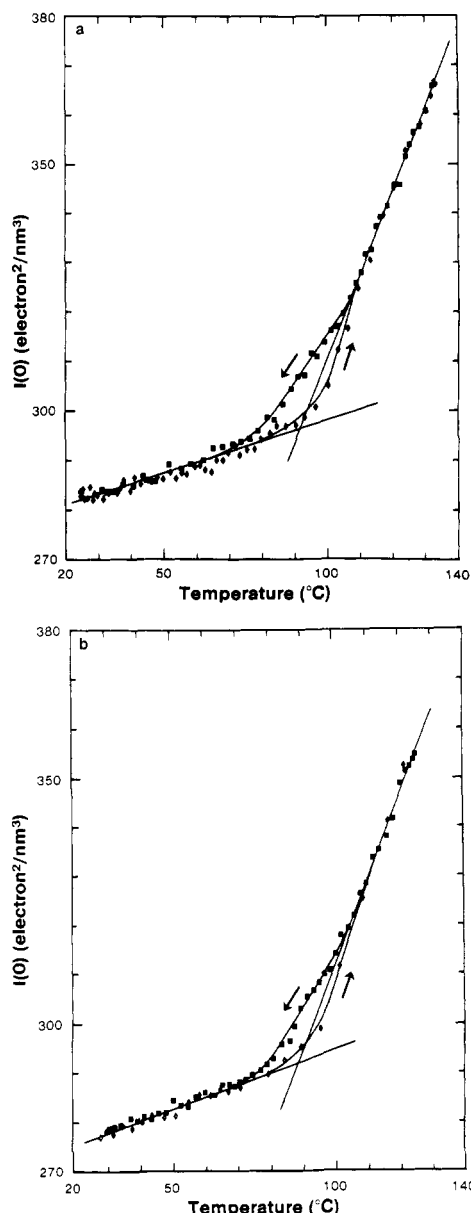


Figure 2. Intensity $I(0)$, corrected for slit-smearing effect and extrapolated to zero angle, is plotted against temperature. The filled square was obtained on cooling the sample at the rate of $0.3^\circ\text{C}/\text{min}$, and the open diamond on heating it at $0.5^\circ\text{C}/\text{min}$. (a) 233 000 molecular weight fraction; (b) commercial sample.

to 0 K, the intercepts obtained are 221, -40, and -324 electrons $^2/\text{nm}^3$, respectively. Thus, none of the three linear sections can be approximated by a relation implying a direct proportionality to temperature.

In Figure 4, the observed density fluctuation, evaluated by dividing $I(0)$ by electron density, is compared with the expected dynamic density fluctuation calculated from the compressibility data 17,18 by means of eq 8 and 10. Agreement between the observed and calculated values above T_g is very good—in fact better than expected in view of the experimental difficulties in the determination of both $I(0)$ and compressibility. Below T_g , however, a large difference exists between the observed density fluctuation and the calculated dynamic fluctuation. According to our view that the density fluctuation in glasses consists of dynamic and quasi-static components, the difference between the observed and calculated values can be considered to represent the quasi-static density fluctuation. The major part of the frozen-in fluctuation is acquired while the sample is cooled through the glass transition region.

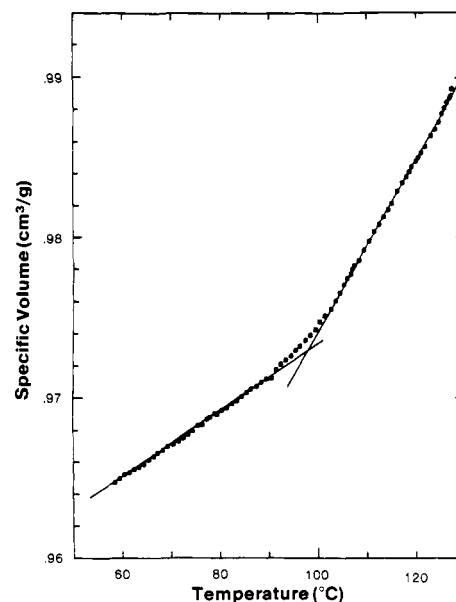


Figure 3. Plotted against temperature is the specific volume of the 233 000 molecular weight fraction, determined by dilatometry on cooling the sample at the rate of $0.3^\circ\text{C}/\text{min}$.

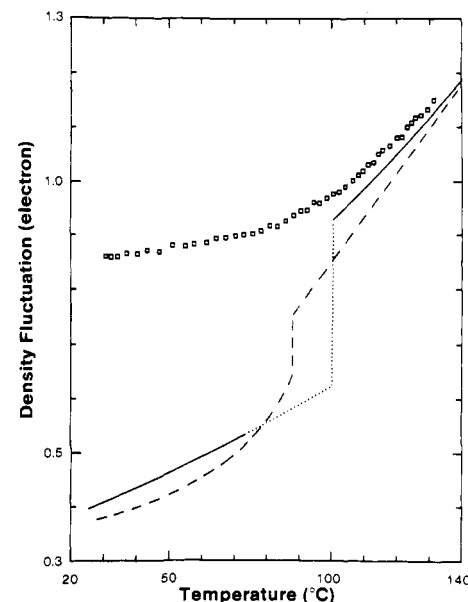


Figure 4. Squares represent the density fluctuation of the 233 000 molecular weight fraction obtained by dividing $I(0)$ (observed on cooling) by electron density. The solid line gives the density fluctuation calculated according to eq 8 and 10 from the compressibility data of Quach and Simha. 18 The broken line shows the density fluctuation calculated similarly from the compressibility data of Hellwege, Knappe, and Lehmann. 17

However, even at temperatures much below T_g , the observed and calculated density fluctuations in Figure 4 continue to diverge with decrease in T . This observation suggests that in glasses further freezing in of degrees of freedom continues with decreasing temperature and more of the dynamic fluctuations are converted into the quasi-static component. The time scale of measurement of the compressibility is probably very much longer than the time scale we employed for the density fluctuation measurement, and therefore a detailed comparison between the two may not be warranted, but the important features deduced from Figure 4 are likely to be valid despite the difference in the time scale.

Figure 5 shows the change in $I(0)$ observed when the samples are annealed isothermally at temperatures below

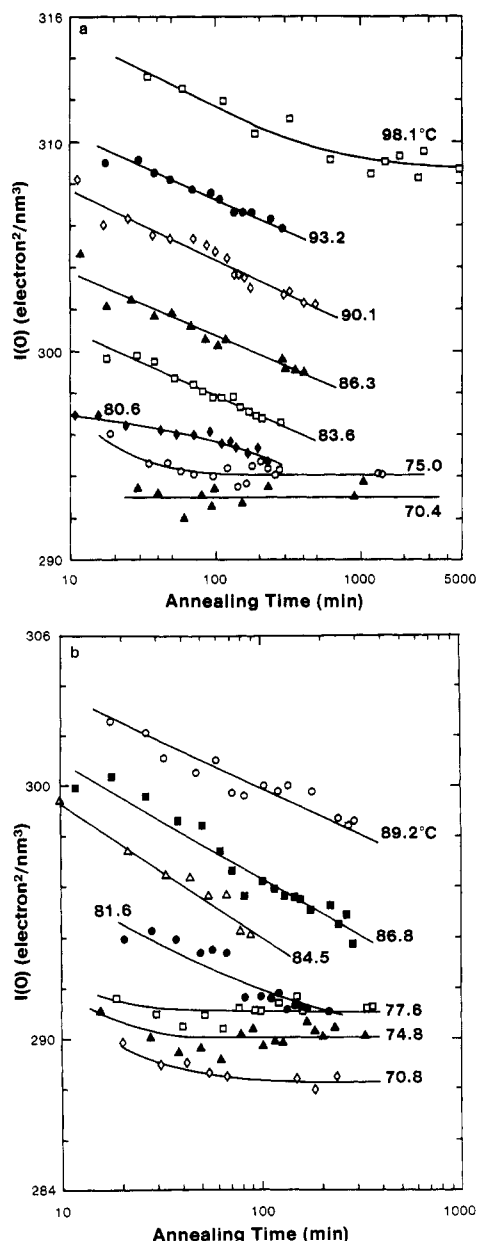


Figure 5. Change in $I(0)$ observed on isothermal annealing at temperatures indicated is shown. (a) 233 000 molecular weight fraction; (b) commercial sample.

T_g . For both the 233 000 molecular weight fraction and the commercial polystyrene, two distinctly different types of pattern are observed, depending on the temperature of annealing. Above about 80 °C, $I(0)$ decreases approximately linearly with the logarithm of time, while below it $I(0)$ remains constant for the duration of observation, which extends to 24 h in some cases. The changeover from the time-dependent to the apparent time-independent behavior occurs over a narrow temperature range of at most several degrees around 80 °C. This temperature agrees fairly well with the temperature in Figure 2a,b at which the straight lines representing the T_g transition region and the glassy region intersect.

The decrease in the specific volume on isothermal annealing, observed by dilatometry, is shown in Figure 6. At all the annealing temperatures investigated, ranging from 99.2 to 61.3 °C, the plot of the specific volume against the logarithm of time is approximately linear. Although one can discern a subtle change in the curvature of the plot with change in the temperature, there is no indication of a gross change in the volume relaxation behavior at around

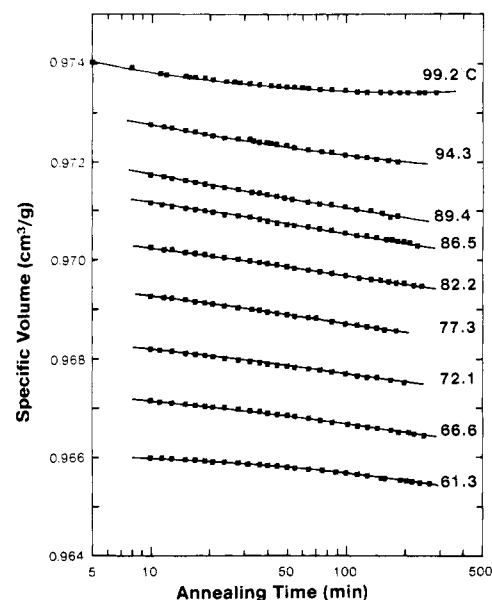


Figure 6. Change in the specific volume of the 233 000 molecular weight fraction, observed by dilatometry on isothermal annealing at temperatures indicated is shown.

80 °C corresponding to the fairly abrupt change observed with the relaxation of the density fluctuation shown in Figure 5. Thus, the difference between the density fluctuation and specific volume observed on constant-rate cooling, shown in Figures 2 and 3, is essentially corroborated by the isothermal relaxation behaviors.

Of the decrease in $I(0)$ observed on annealing, questions arise whether it is the dynamic or quasi-static fluctuation that is decreasing and also in what way it might be related to the volume densification. There is unfortunately no means of separating the total observed $I(0)$ into its components at present. Adopting some plausible assumption relating specific volume and compressibility, we make an attempt at estimating the change in the dynamic density fluctuation associated with the observed change in specific volume. When pressure is increased, both specific volume and compressibility decrease. Similarly, even when the volume is densified as a result of relaxation of the glass structure instead of an increase in pressure, the compressibility might still decrease. In the absence of any other information, we here make the assumption that the compressibility at a given temperature is related to the specific volume uniquely irrespective of how the volume change is induced. We then utilize the data available in the literature^{17,18} on the effect of pressure on compressibility. According to Quach and Simha¹⁸ the Tait equation

$$1 - V/V_0 = 0.0894 \ln [1 + P/B(T)] \quad (13)$$

represents the volume-pressure data well both above and below T_g . It then follows that

$$d \ln \beta_T / d \ln V \approx 1/0.0894 \quad (14)$$

Figure 6 shows that at 86.5 °C, for example, the specific volume decreased by 0.00061 cm³/g during the time period of 20–200 min of annealing. The corresponding decrease in the dynamic component of $I(0)$, equal to $\rho^2 k T \beta_T$, calculated according to eq 29 would be about 1.1 electrons²/nm³. The observed change in $I(0)$ at 86.3 °C, shown in Figure 5a, during the same period of annealing is about 3.1 electrons²/nm³. It therefore suggests that the observed decrease in $I(0)$ on annealing cannot be associated with the volume densification alone. The total change in $I(0)$ on

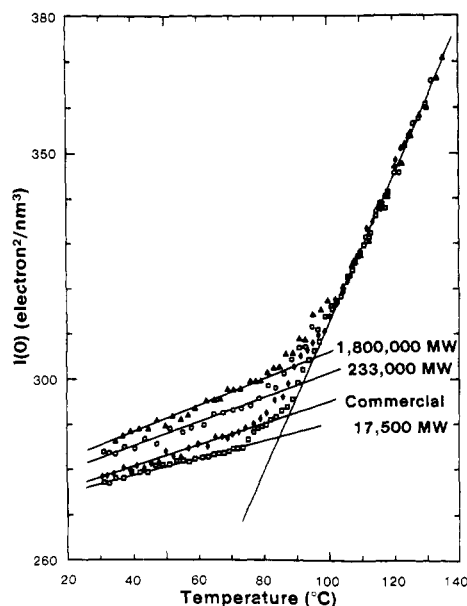


Figure 7. Values of $I(0)$ obtained with four different samples (on constant-rate) cooling) are plotted to show the effect of molecular weight on the density fluctuation of polystyrene glasses.

annealing must have contributions from both the dynamic and quasi-static fluctuations, the former associated with volume densification and the latter with structural reorganization and consequent elimination of some of the frozen-in defects.

Below about 80 °C, the observed $I(0)$ apparently remains constant with time on isothermal annealing. Although prolonged annealing might indeed produce a change in $I(0)$, the particular mode of relaxation that gave rise to a decrease in $I(0)$ with annealing above 80 °C has now been almost totally arrested. On the other hand, the volume relaxation evidently proceeds at about the same rate both above and below the "transition" temperature 80 °C. In order to reconcile these observations we speculate that the fraction of dynamic fluctuation lost as a result of the decrease in compressibility may not simply disappear but instead is converted into a frozen quasi-static fluctuation. The notion of a sharp distinction between dynamic and quasi-static fluctuations, based on the concept of "ideal" glass structure, is, of course, a simplification and there certainly exists in reality a spectrum of density fluctuations of different relaxation times. Thus, a conversion of some of the components of fluctuations with annealing from a dynamic to a quasi-static category would correspond to a gradual change in the relaxation time spectrum of the density fluctuation.

The level of the frozen-in quasi-static fluctuation is sensitive to the molecular weight of the polymer. This is shown in Figure 7, where the $I(0)$ values determined at the cooling rate of 0.3 °C/min for four different polystyrene samples are compared. For the 1 800 000 molecular weight fraction the $I(0)$ value in the glassy state is about 2% higher than the value for the 17 000 molecular weight fraction. The specific volume of polymer glasses is known to be fairly insensitive to molecular weight. Richardson and Savill¹⁸ performed careful dilatometric measurements on a series of narrow polystyrene fractions obtained from the same commercial source as our samples. According to their results, the effect of molecular weight on the specific volume at room temperature for the molecular weight range of interest here is insignificant and entirely within the experimental error. Their results also show that the glass transition temperatures, determined as the intersection of the linear extrapolations of specific volumes

in the liquid and glass regions, are 93.4, 92.9, and 87.9 °C for the fractions with molecular weight 1 990 000, 193 000, and 19 800, respectively. In comparison, the similar intersections of $I(0)$ values in Figure 7 show a larger difference in the apparent T_g among the three fractions having closely corresponding molecular weight.

In the above it has been shown that the volume and the density fluctuation behave very differently on constant-rate cooling, on isothermal annealing, and with respect to their dependence on molecular weight. Structural relaxation in glassy polymers probably proceeds through a number of distinct molecular processes occurring simultaneously. A measuring technique yields an observed value that reflects these various molecular processes, each weighted according to the sensitivity of the technique to that process. The clear difference observed between the behavior of volume and density fluctuation thus indicates that these two properties provide information on very different types of molecular processes. In the language of order parameters frequently employed for the description of glasses,^{20,21} the thermodynamic state of a nonequilibrium system is specified by a set of order parameters $\{Z_n\}$ in addition to T and p . A macroscopic property is then given as $\phi_i(\{Z_n\}, T, p)$, the functional dependence ϕ_i on $\{Z_n\}$ being unique to each property. A change in the said property with time is then given by $\sum_n (\partial \phi_i / \partial Z_n) (dZ_n / dt)$. If it happens that only one order parameter is sufficient to describe the nonequilibrium system, the kinetics of relaxation of one macroscopic property, given by $(d\phi_i / dZ_i) (dZ_i / dt)$, will be identical with those of any other properties. The fact that the volume and density fluctuation follow kinetics very different from each other shows that a number of order parameters are required to represent the polystyrene glasses studied here. The clear difference in the relaxation characteristics between the volume and the density fluctuation shows that each of these two properties in effect reflects a fairly distinct set of order parameters (or molecular processes).

An intuitive understanding of the difference between the behaviors of the volume and the density fluctuation can be obtained if we regard the specific volume as representing the average free volume and the density fluctuation the distribution of free volume in space. In the language of "holes", one might also say that the specific volume represents the density of holes and the density fluctuation the spatial distribution of these holes. It is then not difficult to contemplate physical models in which the average and the distribution of free volume do not always change in parallel when the structure as a whole undergoes a slow relaxation. A simple example of such models was already discussed in an earlier paper²¹ by one of us.

The concept of free volume has in the past proven to be extremely useful in explaining the gross behavior of glass, including the relaxations of volume, enthalpy, and mechanical properties. More recently, however, it has increasingly been recognized that the concept of free volume alone is not sufficient to explain the details of observed phenomena, and instead the concept of distribution of free volume and its change with time are additionally invoked.^{3,22} The results presented in this work show that the density fluctuation, which can be interpreted as a measure of the distribution of free volume, can readily be determined in practice by means of small-angle X-ray scattering. The density fluctuation provides glimpses into the complex structure of glassy materials that are very different from those provided by volume, enthalpy, and mechanical properties, and its detailed study is likely to play an important role in our quest for the understanding

of the nature of the glassy state.

Acknowledgment. This work was supported in part by NSF Grant DMR 80-04236.

Appendix

A derivation of eq 6 is given here. The natural choice for the reference volume v , to be used in eq 4, would be a sphere, within which the form factor equals unity and without which it equals zero. The Fourier transform of such a form factor decays slowly with increasing s (approximately as s^{-4}). As a result the integral in eq 4, with $I(s)$ given by eq 5, diverges. The divergence can, of course, be avoided if we use a realistic $I(s)$ for larger s , since eq 5 obviously grossly overestimates the true scattered intensity at large s . An alternate, approximate method is to use a form factor that does not drop abruptly from unity to zero at its boundaries. We adopt the following form factor:

$$\Sigma(r) = 2^{3/2} \exp(-1/2 r^2 / \sigma^2) \quad (\text{A1})$$

Its volume is given by

$$v = \int \Sigma(r) (4\pi r^2) dr = (2\pi^{1/2} \sigma)^3 \quad (\text{A2})$$

and its Fourier transform by

$$\Phi(s) = (2\pi^{1/2} \sigma)^3 \exp(-2\pi^2 \sigma^2 s^2) \quad (\text{A3})$$

The normalization constant $2^{3/2}$ for $\Sigma(r)$ is given by the requirement that

$$(1/v) \int \Phi^2(s) (4\pi s^2) ds = 1$$

Substitution of (A3) and (5) into eq 4 then leads to eq 6 shown.

References and Notes

- (1) Kovacs, A. J. *Fortschr. Hochpoly. Forsch.* **1963**, *3*, 394.
- (2) Petrie, S. E. B. *J. Polym. Sci., Part A* **1972**, *10*, 1255.
- (3) Struik, L. C. E. "Physical Aging in Amorphous Polymers and Other Materials"; Elsevier: Amsterdam, 1978.
- (4) Guinier, A.; Fournet, G. "Small-Angle Scattering of X-rays"; Wiley: New York, 1955.
- (5) Wendorff, J. H.; Fischer, E. W. *Kolloid Z. Z. Polym.* **1973**, *251*, 876, 884.
- (6) Renninger, A. L.; Wicks, G. G.; Uhlmann, D. R. *J. Polym. Sci., Polym. Phys. Ed.* **1975**, *13*, 1247.
- (7) Renninger, A. L.; Uhlmann, D. R. *J. Polym. Sci., Polym. Phys. Ed.* **1975**, *13*, 1481; **1976**, *14*, 415; **1978**, *16*, 2237.
- (8) Straff, R. S.; Uhlmann, D. R. *J. Polym. Sci., Polym. Phys. Ed.* **1976**, *14*, 353.
- (9) Matyi, R. J.; Uhlmann, D. R.; Koutsky, J. A. *J. Polym. Sci., Polym. Phys. Ed.* **1980**, *18*, 1053.
- (10) Ruland, W. *Prog. Colloid Polym. Sci.* **1975**, *57*, 192.
- (11) Rathje, J.; Ruland, W. *Colloid Polym. Sci.* **1976**, *254*, 358.
- (12) Wiegand, W. Inaugural-Dissertation, Marburg/Lahn, 1977.
- (13) Edwards, S. F. *Polymer* **1976**, *17*, 933. *Ann. N.Y. Acad. Sci.* **1981**, *371*, 210.
- (14) Roe, R.-J., submitted for publication.
- (15) Roe, R.-J.; Chang, J. C.; Fishkis, M.; Curro, J. J. *J. Appl. Crystallogr.* **1981**, *14*, 139.
- (16) Kratky, O.; Pilz, I.; Schmitz, P. J. *J. Colloid Interface Sci.* **1966**, *21*, 24.
- (17) Hellwege, K.-H.; Knappe, W.; Lehman, P. *Kolloid Z. Z. Polym.* **1962**, *183*, 110.
- (18) Quach, A.; Simha, R. *J. Appl. Phys.* **1971**, *42*, 4592.
- (19) Richardson, M. J.; Savill, N. G. *Polymer* **1977**, *18*, 3.
- (20) Davies, R. O.; Jones, G. O. *Adv. Phys.* **1953**, *2*, 370.
- (21) Roe, R.-J. *J. Appl. Phys.* **1977**, *48*, 4085.
- (22) Robertson, R. E. *J. Polym. Sci., Polym. Symp.* **1978**, No. 63, 173.

Experimental Measurements of the Temporal Evolution of Cluster Size Distributions for High-Functionality Antigens Cross-Linked by Antibody

Gustav K. von Schulthess and George B. Benedek*

Department of Physics and Center for Materials Sciences and Engineering, Massachusetts Institute of Technology, Cambridge, Massachusetts 02139

Ralph W. De Blois

General Electric Research Laboratories, Schenectady, New York 12345.
Received May 25, 1982

ABSTRACT: Using a very sensitive Nanopar resistive pulse analyzer, we have been able to determine the temporal evolution of the cluster size distributions produced by bivalent antibodies cross-linking 0.235- μm polystyrene spheres coated with antigen. If X_n is the mole fraction of clusters containing n spheres and X_0 the mole fraction of spheres initially added, then it is found that the cluster size distributions are determined solely by the bonding parameter $b \equiv 1 - \sum X_n / X_0$. We report here the dependence of b upon the time t , the cross-linking antibody concentration $[\text{ab}]_0$, and X_0 , the sphere concentration. We have compared these results for $b(t)$ and our previously reported form of the cluster size distribution $X_n / X_0 = (1 - b)(be^{-b})^{n-1} / bn!$ with extant statistical and kinetic theories.

Introduction

The formation of a distribution of various size clusters through the interaction between initially distinct units is a central feature of widely diverse processes in chemistry, biology, and physics. Examples of these are polymerization processes in organic chemistry, antibody-antigen binding in immunology, coagulation processes in aerosol and colloid physics, phase transitions in disordered magnetic

spin systems, and percolation processes in statistical physics.

Two viewpoints have been taken to describe the temporal evolution of the cluster size distributions. In the first, the temporally evolving distributions are described by means of a set of coupled differential equations: the Smoluchowski equations,¹ whose coefficients, the bimolecular reaction rate coefficients $a_{nn'}$, depend upon the